Inorganic Chemistry

Article

pubs.acs.org/IC

$NH_4FeCl_2(HCOO)$: Synthesis, Structure, and Magnetism of a Novel Low-Dimensional Magnetic Material

Joshua T. Greenfield, Saeed Kamali, Nezhueyotl Izquierdo, Michael Chen, and Kirill Kovnir*

Department of Chemistry, University of California, Davis, One Shields Avenue, Davis, California 95616, United States

Supporting Information

ABSTRACT: Solvothermal synthesis was used to create a low-dimensional iron(II) chloride formate compound, $NH_4FeCl_2(HCOO)$, that exhibits interesting magnetic properties. $NH_4FeCl_2(HCOO)$ crystallizes in the monoclinic space group $C2/c$ (No. 15) with a = 7.888(1) Å, b = 11.156(2) Å, c = 6.920(2) Å, and β = 108.066(2)°. The crystal structure consists of infinite zigzag chains of distorted Fe^{2+}-centered octahedra linked by μ_2-Cl and syn-syn formate bridges, with interchain hydrogen bonding through NH_4^+ cations holding the chains together. The unique Fe^{2+} site is coordinated by four equatorial chlorides at a distance of 2.50 Å and two axial oxygens at a distance of 2.08 Å. Magnetic measurements performed on powder and oriented single-crystal samples show complex anisotropic magnetic behavior dominated by antiferromagnetic interactions (T_N = 6 K) with a small ferromagnetic component in the direction of chain propagation. An anisotropic metamagnetic transition was observed in the ordered state at 2 K in an applied magnetic field of 0.85−3 T. ^{57}Fe Mössbauer spectroscopy reveals mixed hyperfine interactions below the ordering temperature, with strong electric field gradients and complex noncollinear arrangement of the magnetic moments.

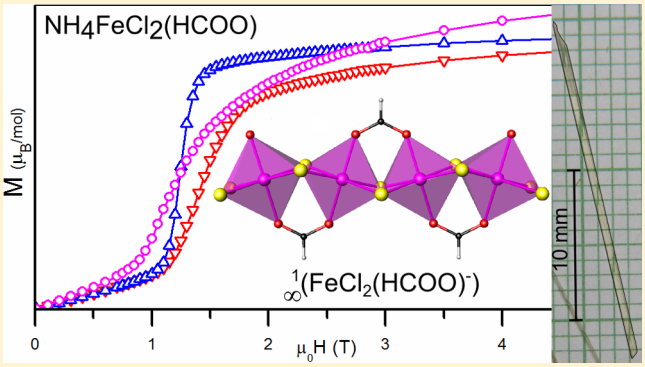

INTRODUCTION

The anisotropy inherent in low-dimensional (1-D) solid-state compounds leads to a variety of interesting magnetic, electronic, and optical properties, with applications including single-chain magnets for data storage,[1] multiferroics for bifunctional materials,[2,3] and nonlinear optical materials for second harmonic generation.[4,5] Certain types of 1-D materials containing isolated chains exhibit nearly ideal magnetic properties, acting as experimental models for Ising and Heisenberg spin chains, furthering our understanding of magnetic exchange in highly correlated systems.[6] One of the strategies for building these 1-D magnetic materials is to incorporate small one- or three-atom linkers between magnetic centers to facilitate exchange along the chains or networks.[7,8] Many of these compounds are known, but very few have been created using iron centers, and most rely on relatively large bridging ligands to separate the magnetically coupled components within the structure. Presented here is the novel compound $NH_4FeCl_2(HCOO)$, containing infinite chains of Fe^{2+}-centered octahedra connected in a zigzag pattern by μ_2-Cl and syn-syn formate bridging ligands. We have characterized this compound with single-crystal and powder X-ray diffraction, direct current (DC) superconducting quantum interference device (SQUID) magnetometry, and ^{57}Fe Mössbauer spectroscopy, revealing antiferromagnetic ordering at 6 K, strong electric field gradients, complex noncollinear antiferromagnetic coupling within the chains, and anisotropic metamagnetic behavior in the ordered state.

EXPERIMENTAL SECTION

Synthesis. *Warning: Solvothermal reactions generate high pressures, and those involving iron and formic acid are capable of producing hydrogen gas, which may result in an explosion. All reactions should be performed in suitable high-strength vessels, and the concentration of formic acid should be kept to a minimum.*

Single-phase samples of $NH_4FeCl_2(HCOO)$ were prepared using a solvothermal method. Iron(II) chloride tetrahydrate (Alfa Aesar, 98%), ammonium chloride (Alfa Aesar, >99.5%), formic acid (Acros Organics, 99%), and ethanol (Koptec, >99.5%) were used as received. To produce the largest single crystals, $FeCl_2{\cdot}4H_2O$ (0.5 g, 2.5 mmol), NH_4Cl (0.3 g, 5.6 mmol), and HCOOH (7.5 mL, 0.2 mol) were mixed well in a 45 mL poly(tetrafluoroethylene) (PTFE)-lined stainless steel acid digestion vessel (Parr Instrument Company). Ethanol (22.5 mL) was added to achieve a filling fraction of 67%. The vessel was sealed tightly and heated for 2 d; the temperature was held at 200 °C for the first 24 h, followed by slow cooling to room temperature at a rate of ∼8 °C per hour. The products were filtered and washed with ethanol, yielding large pale-yellow needle-like crystals up to 0.6 × 0.3 × 30 mm^3 (Figure 1 inset). Polycrystalline samples of $NH_4FeCl_2(HCOO)$ can be produced by stirring an identical reaction mixture in a flask at room temperature and ambient pressure; a pale-yellow solid precipitates from the solution within 10 min.

Characterization. *Single Crystal X-ray Diffraction.* Data were collected at 90 K using a Bruker Apex Duo diffractometer with graphite-monochromated Mo Kα (λ = 0.71073 Å) radiation. The data set was recorded as ω-scans (0.3° frame width) and integrated with the Bruker SAINT software package, indexed in a C-centered monoclinic

Received: December 30, 2013
Published: February 26, 2014

   dx.doi.org/10.1021/ic403173v | *Inorg. Chem.* 2014, 53, 3162−3169

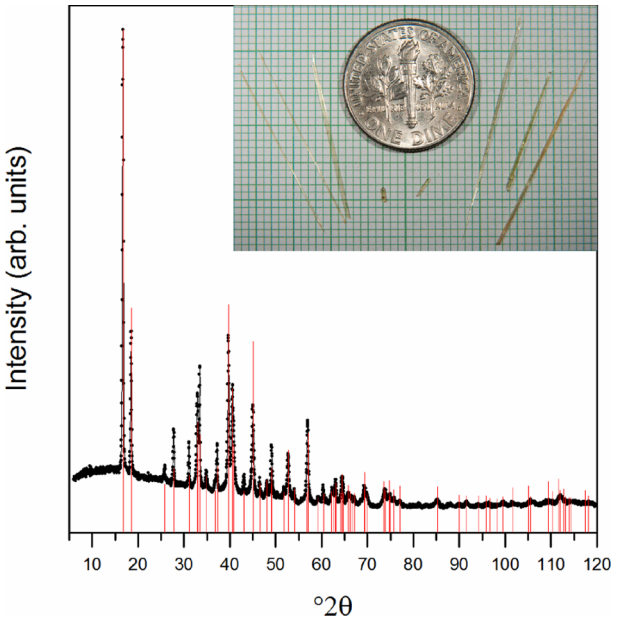

Figure 1. Room-temperature powder X-ray diffraction pattern for powdered single crystals of $NH_4FeCl_2(HCOO)$, λ = 1.7902 Å (Co Kα); experimental data: black circles; calculated peaks (>2% total intensity): red lines. (inset) Single crystals on a 1 mm grid.

unit cell. Analytical absorption correction was applied from the face-indexing of the crystal. The solution and refinement were carried out using the SHELX suite of programs.[9] The structure was solved in space group $C2/c$ (no. 15), with the final refinement performed using anisotropic atomic displacement parameters for all atoms except hydrogen, which were refined isotropically. Pertinent information relating to data collection, unit cell parameters, and structure refinement is summarized in Table 1, and selected interatomic distances and angles are provided in Table 2.

Table 1. Single Crystal Data Collection and Structure Refinement Parameters for $NH_4FeCl_2(HCOO)$[a]

space group	$C2/c$ (no. 15)	θ (deg)	$3.27 < \theta < 32.49$
temp. (K)	90(2)	Z	4
a (Å)	7.888(1)	ρ (g cm^{-3})	2.178
b (Å)	11.156(2)	μ (mm^{-1})	3.417
c (Å)	6.920(2)	data/param	1021/44
β (deg)	108.066(2)	R_1	0.015
V (Å^3)	578.9(2)	wR_2	0.040
λ (Å)	0.71073 (Mo Kα)	goodness-of-fit	1.086

[a]Further details may be obtained from the Cambridge Crystallographic Data Centre by quoting the depository number CCDC-978883.

Table 2. Selected Interatomic Distances and Angles for $NH_4FeCl_2(HCOO)$

atoms	distance (Å)	atoms	angle (deg)
Fe−Cl^{a,c}	2.5003(5)	Cl^a−Fe−Cl^b	87.47(2)
Fe−Cl^{b,d}	2.4996(4)	Cl^b−Fe−Cl^c	92.53(2)
Fe−O	2.0791(8)	O−Fe−Cl^a	90.82(2)
		O−Fe−Cl^b	88.96(2)
N−H···O	2.879(1)	N−H−O	172.5(2)
H···O	1.987(2)		
N−H···Cl	3.385(1)	N−H−Cl	152.3(2)
H···Cl	2.58(2)		

X-ray Powder Diffraction. Samples were characterized by powder X-ray diffraction (PXRD) in the range $5° < 2\theta < 120°$ using an Inel diffractometer employing Co Kα radiation (λ = 1.7902 Å). Unit cell refinement was performed with WinCSD Version 08.11,[10] using a rutile TiO_2 internal standard (NBS SRM 674); least-squares refinement of the room-temperature data yielded lattice parameters: a = 7.894(1) Å, b = 11.235(6) Å, c = 6.936(5) Å, and β = 108.53(3)°.

Magnetic Properties. Temperature-dependent magnetic susceptibility (2−300 K, 0.01 T applied field) and isothermal magnetization (2 K, 0−5 T applied field) were measured with a Quantum Design MPMS-XL SQUID magnetometer. Measurements were performed on an oriented single crystal (0.5 × 0.2 × 5.0 mm^3, 1.0 mg), which was face-indexed using a single-crystal X-ray diffractometer. The morphology of the crystal allowed for the application of the magnetic field in three mutually orthogonal directions: parallel to the [001] direction, perpendicular to the (110) plane, and simultaneously parallel to (110) and perpendicular to [001]. Measurements were also performed on a sample of single crystals ground into a fine powder, affixed to a long piece of Kapton tape to minimize diamagnetic sample holder contributions.

Mössbauer Spectroscopy. ^{57}Fe Mössbauer spectra were collected with a conventional constant-acceleration spectrometer equipped with a ^{57}Co/Rh source held at room temperature. Spectra were collected at room temperature and at 5 K for a sample consisting of numerous single crystals with the [001] direction held perpendicular to the incident γ-radiation. Least-squares fitting of the spectra was performed using the Recoil software package,[11] and all centroid shifts (δ) are given with respect to metallic α-iron at room temperature.

RESULTS AND DISCUSSION

Synthesis. Solvothermal synthesis is a versatile technique that grants access to many solid-state materials and has been successfully applied to a wide variety of systems. The first member of the new iron chloride formate family of compounds was discovered during an attempt to synthesize binary iron selenides under solvothermal conditions. The reaction utilized elemental iron and selenium powders, ammonium chloride as a mineralizing agent, and formic acid to further assist in the dissolution of the iron. Under these conditions, formate and chloride anions strongly coordinate iron in a variety of bridging modes, leading to several 1-D structures (*Caution! This reaction also produced a small quantity of highly toxic H_2Se gas*). Performing the reaction in the absence of selenium produced $NH_4FeCl_2(HCOO)$, though in a relatively low yield and with a significant admixture of α-Fe_2O_3. Optimization of the reaction conditions revealed that the use of $FeCl_2{\cdot}4H_2O$ as an iron source led to single-phase samples containing higher yields of much larger crystals. Additionally, it was determined that an excess of both formic acid and ammonium chloride are required for the formation of the target compound; reactions with reduced volumes of formic acid produced significant quantities of α-Fe_2O_3 impurities, and any less than a 2-fold molar excess of ammonium chloride produced only α-Fe_2O_3. Syntheses were also attempted using ammonium formate instead of ammonium chloride and formic acid, but these reactions also led to the complete oxidation of the iron. It was also discovered that polycrystalline samples can be prepared from similar reaction mixtures under ambient conditions, as the product precipitates from the solution as a pale-yellow solid after 10 min of stirring. The phase purity of solvothermally grown crystals and polycrystalline products was confirmed with PXRD, with all experimental peaks closely matching the calculated pattern (Figure 1). While single crystals of the target compound can be produced solvothermally in as little as 18 h (6 h at 200 °C, followed by cooling to room temperature over 12 h), it was

dx.doi.org/10.1021/ic403173v | Inorg. Chem. 2014, 53, 3162−3169

found that slow cooling over a period of 2−5 d results in the largest, highest quality crystals (Figure 1 inset). Most crystals contain a very small black inclusion at one end, suggesting that nucleation occurs on an iron oxide impurity, though these inclusions may be carefully trimmed off. Reducing the reaction temperature to 150 °C virtually eliminated the formation of iron oxide, but also resulted in much smaller crystals.

Crystal Structure. The structure of $NH_4FeCl_2(HCOO)$ consists of infinite linear chains of distorted edge-sharing octahedra propagating along the crystallographic *c* direction, as shown in Figure 2, with the needle-like crystals growing along

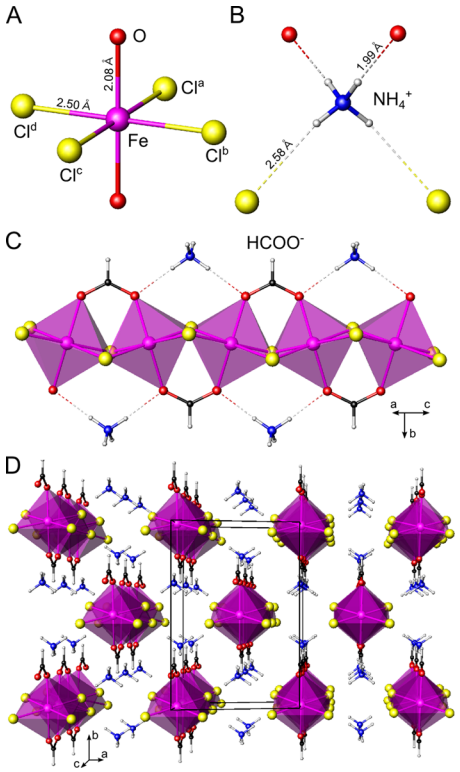

Figure 2. Crystal structure of $NH_4FeCl_2(HCOO)$. (a) Local coordination of Fe^{2+}. (b) Local coordination of NH_4^+. (c) Linear chain. (d) General view. Fe: magenta; Cl: yellow; O: red; N: blue; C: black; H: white.

the direction of chain propagation. Each octahedron is centered on an iron atom that is coordinated by four chlorides in equatorial positions and two oxygens from separate formate ligands in axial positions (Figure 2a). These octahedra cannot be approximated as having regular local $m3m$ (O_h) symmetry, as several distortions lower the symmetry to 222 (D_2). A Jahn−Teller distortion appears as a flattening of the octahedra along the axial direction due to the length difference between Fe−Cl (2.50 Å) and Fe−O (2.08 Å) bonds, reducing the symmetry to $4/mmm$ (D_{4h}). Furthermore, the ideally square-planar $FeCl_4$ moiety is elongated into a rectangle; along the shared edges within the chain, the angle $\angle Cl^a–Fe–Cl^b$ is 87.5°, whereas on the unshared edges the angle $\angle Cl^b–Fe–Cl^c$ is 92.5°. Additionally, the formate anions are rotated 2.6° with respect to the chains, such that the angle $\angle O–Fe–Cl^a$ is 90.8° and the angle $\angle O–Fe–Cl^b$ is 89.0°, resulting in a 222 (D_2) local symmetry.

Formate ligands bridge the axial positions of adjacent octahedra in a syn-syn geometry, causing them to tilt toward each other in a zigzag pattern (Figure 2c). The dihedral angle between the equatorial planes in adjacent octahedra is 146.4°, leaving an arrangement of alternating gaps on either side of the chain. These spaces are occupied by ammonium cations, which form a hydrogen bonding network that holds the chains together. The first coordination sphere of the ammonium cations (Figure 2b) can be approximated as a strongly distorted tetrahedron. The primary interactions are strong hydrogen bonds with formate oxygens, with a N−H···O bond of 2.88 Å and an angle ∠N−H−O of 172.6°. This accounts for two of the four ammonium hydrogens, and plays the largest role in orienting the cation with respect to the chain. The remaining hydrogens interact more weakly with chlorides of two additional chains, with a shortest N−H···Cl distance of 3.39 Å and an angle ∠N−H−Cl of 152.3°. These interactions position the chains relative to each other, resulting in the overall packing shown in Figure 2d.

The linear chains in $NH_4FeCl_2(HCOO)$ resemble those found in a number of previously reported structures incorporating iron, chloride, or formate, but never the combination of the three, as shown in Figure 3. The simplest related structure is that of $FeCl_2·2H_2O$[12] (Figure 3a), in which the octahedral coordination of Fe^{2+} is completed by oxygen from water instead of formate, and the ammonium counterion is absent. In this structure the iron octahedra are more symmetric, but still somewhat distorted; there are two sets of Fe−Cl distances (2.46 and 2.50 Å), and intrachain angles $\angle Cl^a–Fe–Cl^b$ are similarly reduced from the ideal 90° to 87°, though the angle ∠O−Fe−Cl remains 90°. A step closer to the present compound is $FeCl_2(phen)$,[13] in which 1,10-phenanthroline (phen) is employed as a coordinating ligand in place of formate anions (Figure 3b). However, its bulky nature prevents it from bridging adjacent octahedra, and as such it occupies two positions for each Fe^{2+}. This leads to a similar zigzag arrangement but with only the μ_2-Cl bridges. A different type of structure is known for compounds with only formate linkers, as the variety of modes with which the formate anion can bind leads to extended three-dimensional frameworks.[14−17] Figure 3c shows one of the chains present in $[Fe(HCOO)_2]·(1/3)HCOOH$,[18] with interchain linkages omitted for clarity. In this compound, one of the formate ligands bridges the axial positions of the iron octahedra, as is seen in $NH_4FeCl_2(HCOO)$, but two additional formates replace the μ_2-Cl bridges; as only one of the formate oxygens acts as a μ_2-bridge, the other is free to interact with adjacent chains, linking them in three dimensions.

Mixed-bridge chains similar to those in $NH_4FeCl_2(HCOO)$ have been observed in a number of previously reported compounds, though very few incorporate iron and most are constructed from larger carboxylate bridges.[4,5,19−21] The two most closely related compounds are $NH_4MnCl_2(OAc)$[22] and $[Fe(N_3)_2(HCOO)][(CH_3)_2NH_2]$.[23] $NH_4MnCl_2(OAc)$ shares the μ_2-Cl bridges, though the relatively bulky methyl constituent of the acetyl linker (in place of the formate hydrogen) is repulsed by the ammonium cations, causing each to be pushed to one side of the chain, whereas in the present compound the ammonium and formate moieties are coplanar. Despite this difference, the local coordination of the metal and the zigzag nature of the chains are similar, with comparable metal-chloride distances (Fe−Cl = 2.50 Å, Mn−Cl = 2.52−2.63 Å) and octahedral angles (∠Cl−Fe−Cl = 87.5/92.5°, ∠Cl−Mn−Cl = 86.3−96.2°; ∠Cl−Fe−O = 89−91°, ∠Cl−Mn−O = 87.8−91.6°), though the $MnCl_4O_2$ octahedra are more distorted. $[Fe(N_3)_2(HCOO)][(CH_3)_2NH_2]$ is one of the few

dx.doi.org/10.1021/ic403173v | Inorg. Chem. 2014, 53, 3162−3169

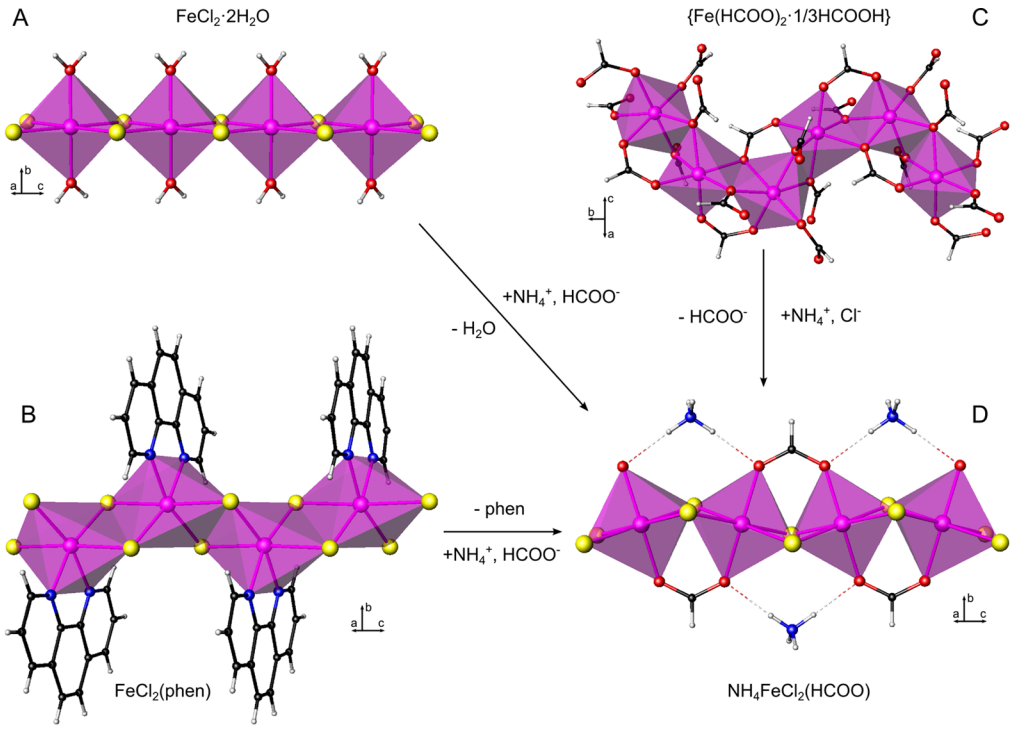

Figure 3. Iron-centered octahedral chains in (a) $FeCl_2·2H_2O$,[12] (b) $FeCl_2(phen)$,[13] (c) $[Fe(HCOO)_2]·(1/3)HCOOH$,[18] and (d) $NH_4FeCl_2(HCOO)$ (this Work). Fe, magenta; Cl, yellow; O, red; N, blue; C, black; H, white.

known compounds containing isolated linear chains of octahedrally coordinated iron, and has the same syn-syn formate bridges, but the μ_2-Cl bridges are replaced by end-on azido ligands. The Fe−N bonds (2.16−2.17 Å) are significantly shorter than the Fe−Cl bonds (2.50 Å) in $NH_4FeCl_2(HCOO)$, and the added bulk of the azido ligands increases the distance between chains, such that the structures of the two compounds are not directly comparable. 1-D compounds containing linear chains exhibit a variety of interesting magnetic properties: $FeCl_2·2H_2O$ exhibits three magnetic phases with metamagnetic transitions between them,[24] $NH_4MnCl_2(OAc)$ orders as a one-dimensional Heisenberg antiferromagnet,[22] and $[Fe(N_3)_2(HCOO)][(CH_3)_2NH_2]$ is a metamagnetic material characterized by ferromagnetic intrachain coupling with weak antiferromagnetic interchain interactions.[23] $NH_4FeCl_2(HCOO)$, though structurally very similar to these compounds, exhibits fascinatingly different magnetic properties.

Magnetism. The 1-D nature of the chains in $NH_4FeCl_2(HCOO)$ leads to highly anisotropic magnetic properties, and the presence of iron allows for further characterization through ^{57}Fe Mössbauer spectroscopy. Figure 4 shows (a) the temperature dependence of magnetic susceptibility, (b) the reduced magnetic susceptibility, and (c) the field dependence of magnetization for a finely ground powder sample and a single crystal oriented in three mutually orthogonal directions with respect to the magnetic field. These directions are shown with reference to one of the linear chains in (d), and include H ∥ [001], H ⊥ (110), and H ∥ (110) and ⊥ [001].

In all four measurements, clear antiferromagnetic ordering was observed with a Néel temperature of 6 K. The ordering temperature is expected to be low, as the zigzag nature of the chains strongly deviates from the linear arrangement necessary for optimal superexchange through the chloride bridges. The peak magnetic susceptibility in an applied magnetic field of 0.01 T varied slightly between the samples, with the H ∥ [001] attaining the highest value, followed by the powder sample, then H ⊥ (110), and finally H ∥ (110) and ⊥ [001]. The reduced magnetic susceptibility demonstrates that this compound deviates slightly from classical antiferromagnetic behavior; in an ideal system the reduced magnetic susceptibility of a single crystal approaches zero for the easy direction of magnetization and remains at a constant maximum value of 1 for the hard direction, while the value for a powder sample approaches 2/3 at 0 K.[25,26] It is apparent that H ∥ [001] is the easiest direction of those observed, but as it does not approach zero, it cannot be the true easy direction; H ⊥ (110) is slightly less favored, and behaves similarly to the powder sample, both of which approach values around 0.4 at 2 K, significantly less than the ideal 0.67. The direction H ∥ (110) and ⊥ [001] appears to be the hardest direction observed, but again it does not behave as the true hard direction for a classical antiferromagnet as its susceptibility also decreases below the ordering temperature. Curie−Weiss fitting of the high-temperature (100−300 K) portion of the data (Figure 4a inset) yields effective magnetic moments ranging from 4.2 to 5.1 μ_B for the oriented single crystal and 5.8 μ_B for the powder sample; these values are typical for high-spin Fe^{2+} ($^5D_4$) with a contribution from spin−orbit coupling.[18,26] The calculated asymptotic Curie temperatures, θ, also reflect significant anisotropy, with values ranging from +18 K for H ∥ [001] to −16 K for the powder sample. The powder sample may have partially oxidized upon pulverization, but the other measurements were performed on the same crystal in the same sample holder. Differing signs of θ between these measurements indicate that even at room temperature $NH_4FeCl_2(HCOO)$ does not behave as an isotropic paramagnet. Data from the powder sample show that the dominant nearest-neighbor interactions in the compound are antiferromagnetic ($-\theta$), and the H ∥ [001] measurement shows a minor ferromagnetic component ($+\theta$) parallel to the c axis, along the direction of chain propagation.

dx.doi.org/10.1021/ic403173v | Inorg. Chem. 2014, 53, 3162−3169

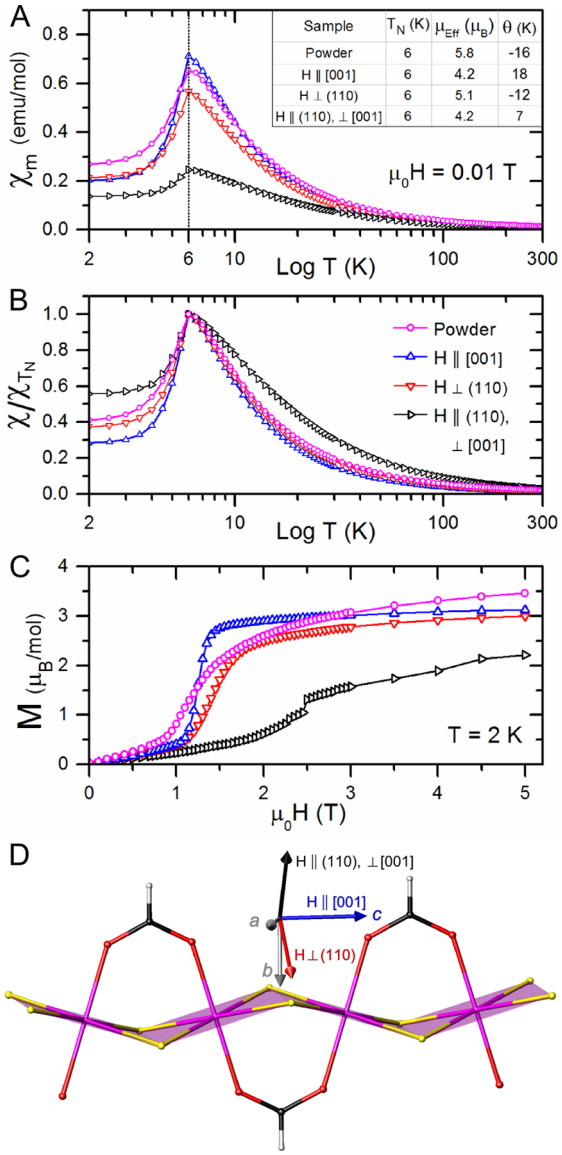

Figure 4. Magnetic measurements for powder and an oriented single crystal of $NH_4FeCl_2(HCOO)$. (a) Temperature-dependent magnetic susceptibility at 0.01 T; inset: parameters calculated from Curie–Weiss fit of high-temperature data; (b) normalized magnetic susceptibility; (c) isothermal magnetization at 2 K; (d) diagram showing applied magnetic field directions. Powder: magenta circle; H ∥ [001]: blue triangle; H ⊥ (110): red triangle; H ∥ (110), ⊥ [001]: black triangle.

This places the magnetic properties of $NH_4FeCl_2(HCOO)$ closer to $[Fe(N_3)_2(HCOO)][(CH_3)_2NH_2]$, which has an antiferromagnetic ground state with strong ferromagnetic interactions within the chains.

The field-dependent magnetization curves at 2 K (Figure 4c) show similar anisotropic behavior, and also reveal metamagnetic transitions in applied fields from 0.85 to 3 T, implying nontrivial magnetic ordering. These fields are significantly higher than the transition observed at 0.2 T in $[Fe(N_3)_2(HCOO)][(CH_3)_2NH_2]$.[23] The measurement with H ∥ [001] shows the sharpest transition, while H ⊥ (001) occurs more gradually, though both orientations have critical fields of 1.1 T and saturate at 3.1 and 3.0 μ_B, respectively. This is likely to arise from the same magnetic transition, with H ∥ [001] closer to the easy axis; however, the transition in the powder sample began at 0.85 T and saturated at 3.46 μ_B, further supporting that none of the measured orientations are the true easy direction. The final orientation, with H ∥ (110) and ⊥ [001], exhibits a much smaller and broader transition between 2 and 3 T; there is a small jump at 2.5 T, and at the highest applied field the moment only reaches 2.2 μ_B, indicating that this orientation is the closest to the hard direction. The magnetization data can also provide some information about the oxidation and spin state of the iron, as the fully saturated magnetic moments should reflect the number of unpaired electrons in each magnetic center. From a simple charge-balance perspective, the formula of the compound could be written as $(NH_4^+)(Fe^{2+})(Cl^-)_2(HCOO^-)$, which places iron in the ferrous state. Ligand-field theory predicts that Fe^{2+} in an octahedral environment of relatively weak-field Cl^- and $HCOO^-$ ligands should have a small Δ_O and therefore exist in the high spin ($S = 2$) state, which would result in a saturated magnetic moment of 4 μ_B. The fact that none of the samples attained this value suggests that the iron centers are more likely to be high-spin Fe^{2+} than Fe^{3+}, and that true collinear ordering cannot be achieved at the measured field strengths and directions.

^{57}Fe Mössbauer spectroscopy was used to further clarify the oxidation and spin state of the iron centers and gain a better understanding of the magnetic ordering in this compound. To examine the properties of both the paramagnetic and antiferromagnetic states, spectra were recorded at room temperature and at 5 K (Figure 5); the fitting results are summarized in Table 3.

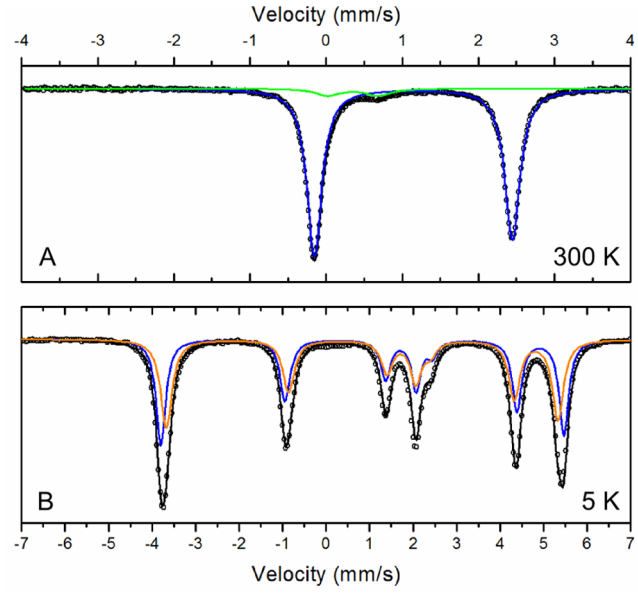

Figure 5. ^{57}Fe Mössbauer spectra of $NH_4FeCl_2(HCOO)$ collected at (a) 300 K and (b) 5 K. Experimental data: black circles; calculated spectrum: black line; $NH_4FeCl_2(HCOO)$ components: blue and orange lines; admixture component: green line.

The room-temperature spectrum can be described by two components: Q_1 and Q_2. Q_1 describes the main feature of the spectrum, a doublet that accounts for 93% of the overall intensity, while Q_2 represents an impurity phase, appearing as a much smaller doublet (7%). The main doublet has a centroid shift (δ) of 1.147 mm/s and an electric quadrupole splitting (ΔE_Q) of 2.60 mm/s. The centroid shift is typical for high-spin

dx.doi.org/10.1021/ic403173v | Inorg. Chem. 2014, 53, 3162–3169

Table 3. Summary of Refined Mössbauer Parameters for 300 and 5 K Spectra

T = 300 K		
	components	
parameters	Q_1	Q_2
δ (mm/s)	1.1470(5)	0.35(2)
ΔE_Q (mm/s)	2.6008(9)	0.67(3)
Γ (mm/s)	0.242(2)	0.38(4)
I (%)	93(1)	7(1)
T = 5 K		
	Q_{1A}	Q_{1B}
δ (mm/s)	1.278(1)	1.279(1)
B_{hf} (T)	25.42(1)	24.65(1)
$e^2qQ/2$ (mm/s)	2.280(2)	2.727(3)
η	0.361(4)	0.392(5)
Γ (mm/s)	0.261(2)	0.313(2)
φ_{Hq} (deg)	45.3(1)	47.0(2)
θ_{Hq} (deg)	79.2(1)	80.1(1)
I (%)	50(1)	50(1)

Fe^{2+},[27,28] consistent with magnetic measurements, and the large quadrupole splitting is an indication of a very high electric field gradient (EFG), likely caused by the significant Jahn−Teller distortion of the iron-centered octahedra. The impurity doublet has a centroid shift (δ) of 0.35 mm/s and an electric quadrupole splitting (ΔE_Q) of 0.67 mm/s, values typical for Fe^{3+} in a high-spin iron oxide, present as small inclusions in the crystals.

The 5 K spectrum is magnetically split, confirming an ordering temperature of 6 K, but the peak positions and intensities indicate that the spectrum is a result of mixed hyperfine interactions, as the high EFG causes quadrupole splitting of roughly the same magnitude as the magnetic hyperfine interaction. In this scenario ΔE_Q can no longer be treated as a perturbation, and a full static Hamiltonian analysis is required.[28,29] This model has been successfully applied to the analysis of similarly split quasi-two-dimensional materials[30] and three-dimensional frameworks containing iron formate chains;[18] in addition to δ, parameters in this model include magnetic hyperfine field ($\mathbf{B}_{hf}$), line width (Γ) and intensity (I), the EFG interaction ($e^2qQ/2$) and asymmetry (η) parameters, and the azimuthal (φ_{Hq}) and polar (θ_{Hq}) angles of $\mathbf{B}_{hf}$ with respect to the principal coordinate axes of the EFG. The corresponding angles φ_{gq} and θ_{gq} between the EFG axes and the incident γ-rays can be calculated, but because of the nature of the sample preparation ([001] held parallel, but a and b axes oriented randomly) these angles average out and cannot be determined. The signal from the high-spin iron oxide impurity seen in the room-temperature spectrum was magnetically split such that the most intense peaks fell far outside the range of interest for our compound, and any peaks present in the same range were of negligible intensity; the remaining discussion is based solely on the signal that corresponds to NH_4FeCl_2(HCOO). Unexpectedly, the only satisfactory least-squares fit with mixed hyperfine interactions can be achieved with two components of equal intensities, Q_{1A} and Q_{1B}. The centroid shift is the same for each component and is consistent with Q_1 from the room-temperature spectrum, with a slightly larger value due to a second-order Doppler shift. However, the values of the other parameters differ, suggesting that there is more than one unique magnetic center. The hyperfine magnetic field is similar for both components, with values of 25.4 T for Q_{1A} and 24.7 T for Q_{1B}, both of which are notably larger than values of 5−15 T reported for a three-dimensional formate framework containing octahedrally coordinated high-spin Fe^{2+} magnetic centers.[18] The EFG interaction parameter shows the greatest difference between the two components, with a value of 2.28 mm/s for Q_{1A} and 2.73 mm/s for Q_{1B}, suggesting that a structural distortion occurs at some temperature below 90 K, causing a difference in the electric field gradient around half of the iron sites.

The model also reveals the relative orientation of the magnetic moments with respect to the EFG; assuming that the shorter Fe−O distance contributes more to the EFG than the longer Fe−Cl bonds, the z axis (the principal coordinate axis of the EFG) will be oriented along the Fe−O bond, and the y axis

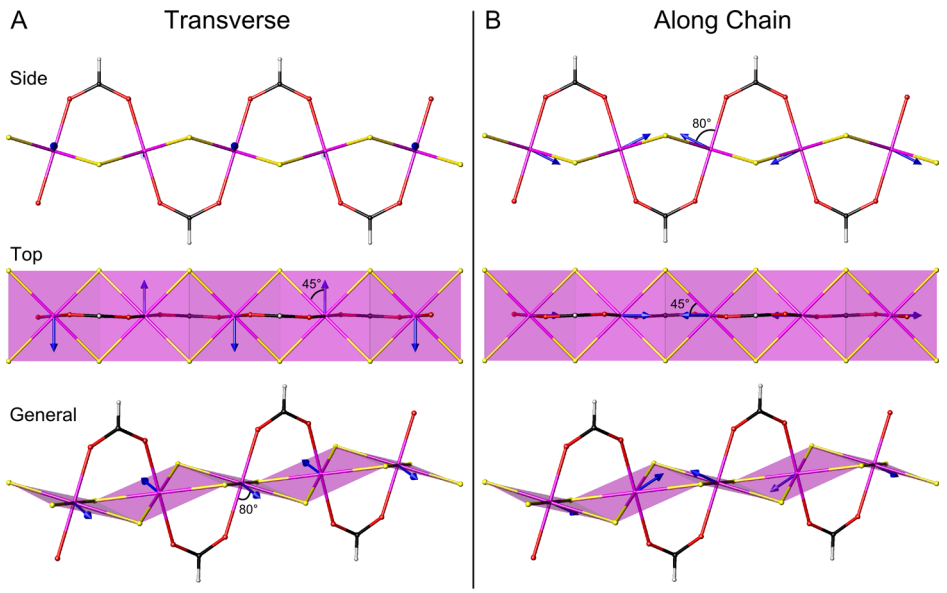

Figure 6. Side, top, and general views of a zigzag chain in two simple magnetic models of NH_4FeCl_2(HCOO). (a) Moments aligned transverse to the chain. (b) Moments aligned along the chain. Magnetic moments shown in blue.

dx.doi.org/10.1021/ic403173v | Inorg. Chem. 2014, 53, 3162−3169

(defined as the next highest contributor) is oriented along one of the Fe−Cl bonds, making the $FeCl_4$ equatorial plane the *xy* plane of the EFG. As the iron centers are in an approximately octahedral environment, the φ_{Hq} and θ_{Hq} parameters reveal that the magnetic moments are oriented roughly 45° from one of the Fe−Cl bonds and 80° from the Fe−O bonds. There are two simple antiferromagnetic models that can be drawn from these angles, as shown in Figure 6. In the first case, the moments are oriented transverse to the direction of the chain, with moments alternating as shown in Figure 6a to maintain a net moment of zero, while in the second case the moments are oriented along the chains, and a more complex arrangement (shown in Figure 6b) is required to maintain antiferromagnetic behavior. Between these two models, the second case is more likely, as it is in better agreement with the magnetization data; the first model would not show a sharp transition when magnetized along the [001] direction, whereas it would be expected of the second model. However, the second model does not predict the drastic difference between the H ⊥ (110) and the H ∥ (110) and ⊥ [001] measurements, showing that the actual arrangement of magnetic moments is more complex. Additionally, given the sample morphology and preparation, the magnetic moments in the second model should lead to a significantly different pattern in the relative intensity of the first two Mössbauer peaks, while the observed intensities are those expected of a randomly oriented (powder) sample. Finally, neither of these models takes into account any interchain interactions that may occur, nor can they treat the as yet unidentified structural distortion that splits the single crystallographic iron position into two distinct magnetic centers. To fully understand the magnetic ordering in $NH_4FeCl_2(HCOO)$, a technique such as low-temperature neutron diffraction is necessary to resolve both the ordered magnetic structure and any magnetostructural distortions that arise with it.

CONCLUSION

In conclusion, we have presented the synthesis, structure, and magnetic properties of a new 1-D magnetic material containing zigzag chains of high-spin Fe^{2+}-centered octahedra bridged by μ_2-Cl and syn-syn formate ligands. This compound exhibits complex magnetic ordering that is dominated by antiferromagnetic interactions, as well as anisotropic metamagnetic transitions. ^{57}Fe Mössbauer spectroscopy reveals mixed hyperfine interactions in the ordered state and suggests that a structural distortion occurs at low temperature to create two crystallographically inequivalent iron positions. The highly anisotropic magnetic properties of $NH_4FeCl_2(HCOO)$ are intriguing, and further studies of this and related compounds are currently underway.

ASSOCIATED CONTENT

Supporting Information

Crystallographic data in CIF format. This material is available free of charge via the Internet at http://pubs.acs.org.

AUTHOR INFORMATION

Corresponding Author

*E-mail: kkovnir@ucdavis.edu. Phone: +1-530-752-5563.

Author Contributions

The manuscript was written through contributions of all authors. All authors have given approval to the final version of the manuscript.

Notes

The authors declare no competing financial interests.

ACKNOWLEDGMENTS

The University of California, Davis and UC Davis ChemEnergy NSF REU Grant #CHE-1004925 are gratefully acknowledged for financial support of this Work. The Mössbauer facility was supported by NIH Grant No. 1S10RR023656-01A1.

REFERENCES

(1) Zhang, W.-X.; Ishikawa, R.; Breedlove, B.; Yamashita, M. *RSC Adv.* **2013**, *3*, 3772−3798.
(2) Xu, G. C.; Ma, X. M.; Zhang, L.; Wang, Z. M.; Gao, S. *J. Am. Chem. Soc.* **2010**, *132*, 9588−9590.
(3) Xu, G. C.; Zhang, W.; Ma, X. M.; Chen, Y. H.; Zhang, L.; Cai, H. L.; Wang, Z. M.; Xiong, R. G.; Gao, S. *J. Am. Chem. Soc.* **2011**, *133*, 14948−14951.
(4) Kandasamy, A.; Siddeswaran, R.; Murugakoothan, P.; Kumar, P. S.; Mohan, R. *Cryst. Growth Des.* **2007**, *7*, 183−186.
(5) Anbuchezhiyan, M.; Ponnusamy, S.; Muthamizhchelvan, C.; Sivakumar, K. *Mater. Res. Bull.* **2010**, *45*, 897−904.
(6) Coulon, C.; Miyasaka, H.; Clerac, R. In *Single-Molecule Magnets and Related Phenomena;* Winpenny, R., Ed.; Springer-Verlag: Berlin, Germany, 2006; Vol. *122*, pp 163−206.
(7) Wang, X.-Y.; Wang, Z.-M.; Gao, S. *Chem. Commun.* **2008**, 281−294.
(8) Sun, H.-L.; Wang, Z.-M.; Gao, S. *Coord. Chem. Rev.* **2010**, *254*, 1081−1100.
(9) Sheldrick, G. M. *Acta Crystallogr.* **2008**, *A64*, 112−122.
(10) Akselrud, L. G. Z.; Yu, P.; Grin, Yu. N.; Pecharski, V. K.; Baumgertner, B.; Wolfel, E. *Mater. Sci. Forum* **1993**, *133−136*, 335−342.
(11) Lagarec, K.; Rancourt, D. G. *Recoil, Mössbauer Spectral Analysis Software for Windows,* Version 1.0; 1998.
(12) Morosin, B.; Graeber, E. J. *J. Chem. Phys.* **1965**, *42*, 898−901.
(13) Sui, X. N.; Lu, X. M.; Feng, J. H.; Wang, S.; Li, P. Z. *J. Coord. Chem.* **2008**, *61*, 1568−1574.
(14) Viertelhaus, M.; Henke, H.; Anson, C. E.; Powell, A. K. *Eur. J. Inorg. Chem.* **2003**, 2283−2289.
(15) Viertelhaus, M.; Anson, C. E.; Powell, A. K. *Z. Anorg. Allg. Chem.* **2005**, *631*, 2365−2370.
(16) Wang, Z. M.; Zhang, B.; Inoue, K.; Fujiwara, H.; Otsuka, T.; Kobayashi, H.; Kurmoo, M. *Inorg. Chem.* **2007**, *46*, 437−445.
(17) Liu, B.; Shang, R.; Hu, K. L.; Wang, Z. M.; Gao, S. *Inorg. Chem.* **2012**, *51*, 13363−13372.
(18) Viertelhaus, M.; Adler, P.; Clerac, R.; Anson, C. E.; Powell, A. K. *Eur. J. Inorg. Chem.* **2005**, 692−703.
(19) Huang, D. G.; Wang, W. G.; Zhang, X. F.; Chen, C. N.; Chen, F.; Liu, Q. T.; Liao, D. Z.; Li, L. C.; Sun, L. C. *Eur. J. Inorg. Chem.* **2004**, 1454−1464.
(20) Ghosh, A.; Dan, M.; Rao, C. N. R. *Solid State Sci.* **2008**, *10*, 998−1005.
(21) Wang, J.-J.; Hu, T.-L.; Bu, X.-H. *CrystEngComm* **2011**, *13*, 5152−5161.
(22) Martin, J. D.; Hess, R. F.; Boyle, P. D. *Inorg. Chem.* **2004**, *43*, 3242−3247.
(23) Liu, T.; Zhang, Y. J.; Wang, Z. M.; Gao, S. *Inorg. Chem.* **2006**, *45*, 2782−2784.
(24) Schneider, W.; Weitzel, H. *Acta Crystallogr.* **1976**, *A32*, 32−37.
(25) Carlin, R. L. *Magnetochemistry;* Springer-Verlag: New York, 1986; Chapter 6.
(26) Buschow, K. H. J.; de Boer, F. R. *Physics of Magnetism and Magnetic Materials;* Kluwer Academic Publishers: New York, 2004; Chapter 2.
(27) Gütlich, P. In *Mössbauer Spectroscopy;* Gonser, U., Ed.; Springer: Berlin Heidelberg, 1975; Vol. *5*, p 53−96.

(28) Gütlich, P.; Ensling, J. In *Ullmann's Encyclopedia of Industrial Chemistry, Electronic Release;* Wiley-VCH: Weinheim, Germany, 2001; Vol. 23, p 607−624.
(29) Blaes, N.; Fischer, H.; Gonser, U. *Nucl. Instrum. Methods Phys. Res., Sect. B* **1985**, *9*, 201−208.
(30) Kamali, S.; Haggstrom, L.; Ronneteg, S.; Berger, R. *Hyperfine Interact.* **2004**, *156*, 315−319.